Gnrh1-induced responses are indirect in female medaka Fsh cells

Kjetil Hodne[+], Romain Fontaine[+], Eirill Ager-Wick, Finn-Arne Weltzien*

Department of Basic Sciences and Aquatic Medicine, Faculty of Veterinary Medicine, Norwegian University of Life Sciences, Oslo, Norway

Short title: Gnrh1-induced responses in Fsh cells are indirect in medaka

[+] These authors contributed equally to this work

* Corresponding author at the above address; Email: finn-arne.weltzien@nmbu.no; Tel: +47 67232036

KEY WORDS: calcium, cell-cell communication, gnrh receptor, gonadotropins, pituitary

FUNDING: Research Council of Norway, Grant no 248828 and 244461, and the Norwegian University of Life Sciences

DISCLOSURE STATEMENT: The authors have nothing to disclose.

ACKNOWLEDGEMENTS: We thank Drs Susann Burow and Rasoul Nourizadeh-Lillabadi for help with development of the medaka transgenic line, tg(*fshb*:DsRed2), and Dr Felix Loosli (Karlsruhe Institute of Technology, Germany) for kindly providing the I-SceI-MCS-leader-Gfp-trailer plasmid.

NOMENCLATURE: We use the following nomenclature: “GnRH” for protein names and “*GnRH*” for gene names in general or in mammals, and “Gnrh” for protein names and “*gnrh*” for gene names in teleost fish.

ABSTRACT

Reproductive function in vertebrates is stimulated by gonadotropin-releasing hormone (GnRH) that controls the synthesis and release of the two pituitary gonadotropins, follicle-stimulating hormone (FSH) and luteinizing hormone (LH). FSH and LH, which regulates different stages of gonadal development, are produced by two different cell types in the fish pituitary, in contrast to mammals and birds, thus allowing the investigation of their differential regulation. In the present work, we show by fluorescent *in situ* hybridization that Lh cells in adult female medaka express Gnrh receptors, whereas Fsh cells do not. This is confirmed by patch clamp recordings and cytosolic Ca^{2+} measurements on dispersed pituitary cells, where Lh cells, but not Fsh cells, respond to Gnrh1 by increased action potential frequencies and cytosolic Ca^{2+} levels. In contrast, both Fsh and Lh cells are able to respond electrically and by elevating the cytosolic Ca^{2+} levels to Gnrh1 in brain-pituitary tissue slices. Using Ca^{2+} uncaging in combination with patch clamp recordings and cytosolic Ca^{2+} measurements, we show that Fsh and Lh cells form homo- and heterotypic networks in the pituitary. Taken together, these results show that the effects of Gnrh1 on Fsh release in adult female medaka is indirect, likely mediated via Lh cells.

INTRODUCTION

In all vertebrates, it is suggested that gonadotropin-releasing hormone (GnRH) is the main stimulator of the synthesis and release of the two pituitary gonadotropins: follicle-stimulating hormone (FSH) and luteinizing hormone (LH). GnRH neurons originate in the preoptico-hypothalamic area, but whereas in mammals they release their neuropeptide to the portal capillary system at the base of the hypothalamus termed the median eminence (1) and further to the gonadotrope cells through the circulation, teleost fish do not display a typical median eminence. Instead, the neurosecretory fibers from the brain project into the *pars distalis* of the pituitary (2). These neurons either directly innervate the different endocrine cells or terminate in the extravascular space, adjacent to blood capillaries surrounding the endocrine cells (2-5). Additionally, whereas FSH and LH are produced by the same pituitary cells in mammals (6), they are produced by two distinct cell types in teleosts (7-10). This makes teleosts useful models to investigate the differential regulation of FSH and LH synthesis and release.

FSH and LH control different stages of gamete development both in mammals and teleost fish, with FSH mainly stimulating follicular development in females and LH regulating final maturation and ovulation (11-15). In mammals, the differential regulation of FSH and LH appears to depend on a pulsatile release of GnRH, with low-frequency pulses favoring FSH response and high-frequency pulses favoring LH response, especially in terms of gonadotropin subunit gene expression (16-18). Activation of GnRH receptors on gonadotrope cells elicit increased cytosolic Ca^{2+} levels ($[Ca^{2+}]_i$) with a subsequent alteration in membrane potential and hormone release by exocytosis. A similar response to Gnrh has been shown also in teleost fish (19-25), although a Gnrh pulsatile or frequency dependent release of gonadotropins has not been demonstrated.

As many as 5 or 6 different Gnrh receptor (Gnrhr) paralogs have be identified in several teleost species, as opposed to 1 or 2 paralogs being present in mammals. The high number of Gnrhr paralogs in fish opens the possibility for differential regulation of Fsh and Lh synthesis and release through differential expression of receptors in the two gonadotrope cell types (26-29).

The importance of GnRH signaling seems to differ for the two gonadotropins. In the infertile natural GnRH mutant (*hpg*) mouse, FSH serum levels are reduced by 50%, while LH levels are non-detectable (30,31). Likewise, in the teleost medaka (*Oryzias latipes*), Gnrh knockout in females prevented ovulation and reduced expression of *lhb*, but did not affect *fshb* expression or follicle development (13). These results suggest that LH cell function is dependent on GnRH stimulation, while adequate FSH synthesis and release may continue in the absence of GnRH. Indeed, some reports suggest that FSH release is more constitutive in nature and closely tied to its synthesis (32), but a detailed model for the differential regulation of FSH and LH is still lacking. In addition to differential regulation by GnRH, precise regulation of FSH and LH release may depend on cell-cell communication. A coordinated GnRH-induced LH release requires communication between LH cells through gap junctions, seemingly in both mammals and teleosts (33,34).

In this work, we addressed the question, does Gnrh1 regulate Fsh cells and Lh cells through similar direct pathways, or via different mechanisms? To answer this question we used transgenic lines to clearly distinguish Fsh cells from Lh cells, toward the following objectives: 1) Determine whether hypophysiotropic Gnrh1 neurons project to Fsh and/or Lh cells in the medaka pituitary, 2) Determine which *gnrhr* paralog(s) are expressed in medaka Fsh and Lh cells, 3) Characterize the Gnrh1-induced electrical and $[Ca^{2+}]_i$ responses of medaka Fsh and Lh cells, and 4) Assess capacity for intercellular signaling between gonadotropes in the medaka pituitary.

96 MATERIALS AND METHODS

97 **Animals**

98 In this paper, we used Japanese medaka (*Oryzias latipes*) wild-type (WT, d-rR strain),
99 and four transgenic lines; tg(*gnrh1*:eGfp) (35), tg(*lhb*:hrGfpII) (36), tg(*fshb*:DsRed2) (this
100 paper), double tg(*lhb*:hrGfpII/*fshb*:DsRed2) (this paper). All fish were maintained on a 14:10
101 hr L:D cycle in a re-circulating system (28ºC, pH 7.6 and conductivity of 800 µS) and fed
102 three times a day with either live brine shrimp or pellets (Gemma, Skretting, Stavanger,
103 Norway). Animal experiments were performed according to the recommendations of the Care
104 and Welfare of Research Animals at the Norwegian University of Life Sciences, and under
105 the supervision of authorized investigators.

106

107 **Generation of tg(*fshb*:DsRed2) and double tg(*lhb*:hrGfpII/*fshb*:DsRed2) transgenic**
108 **lines**

109 The medaka *fshb*:DsRed2 transgenic line, tg(*fshb*:DsRed2), was generated using
110 DsRed2-N1 vector (Clontech, California, USA.), digested by NcoI and NotI restriction
111 enzymes (New England Biolabs, USA) and cloned into I-SceI-MCS-leader-Gfp-trailer
112 plasmid, generating a I-SceI-MCS-leader-DsRed2-trailer vector. The 3833 bp endogenous
113 medaka *fshb* promoter sequence was amplified by PCR using primers (see Table 1) with
114 overhang to KpnI and XhoI and cloned into pGEM-T Easy vector. The vector was then
115 amplified, digested with KpnI and XhoI (New England Biolabs, Massachusetts, USA), and
116 the DNA fragment was purified and cloned into the I-SceI-MCS-leader-DsRed2-trailer
117 vector.

118 One-cell stage medaka embryos were injected using a manual microinjector
119 (Picospritzer III, Parker Automation, Ohio, USA) with 10 µg/µl transgenic vector diluted in
120 0.5x commercial meganuclease buffer (Roche Diagnostics, Basel, Switzerland), and with 1

U/µl meganuclease I-SceI and 0.1% phenol red added just prior to use. Injected fish (F0) were raised to adulthood and incrossed. Embryos were screened for DsRed2 by PCR at 5-6 days post fertilization, to determine founders. F0 founders were then crossed with WT and the resulting offspring (F1) were incrossed. Mature F2 were crossed with WT and F2 fish producing 90-100% Rfp-positive progeny were defined to be homozygous: tg(*fshb*:DsRed2). The identified homozygous F2 fish were incrossed to produce a stable homozygous line. Finally, homozygous tg(*fshb*:DsRed2) were crossed with homozygous tg(*lhb*:hrGfpII) to obtain double tg(*lhb*:hrGfp-II/*fshb*:DsRed2) transgenic animals.

qPCR

Total RNA was isolated from 6 adult female medaka (WT) pituitaries using Trizol (Ambion, USA) and cDNA was prepared from 30 ng total RNA. Specific primers for all target genes (Table 1) were designed with Primer3Plus software and validated based on a series of cDNA dilutions (to assess efficiency and sensitivity) and melting curve analysis (to assess specificity). The qPCR assays were performed as previously described (37) using the LightCycler96 with SYBR Green I (Roche, Switzerland). All qPCR assays were run in duplicate on cDNA diluted 1:5. PCR cycling parameters were 300 s at 95ºC followed by 40 cycles at 95ºC for 10 s, 60ºC for 10 s and 72ºC for 6 s, before melting curve analysis to assess qPCR product specificity. Relative expression levels were calculated as described (37), using the combination of three reference genes (*rna18s*, *rpl7*, *gapdh*), according to RefFinder (38).

Fluorescence *in situ* hybridization

Fluorescence *in situ* hybridization (FISH) for *lhb*, *fshb*, *dsred2*, *gnrhr2a*, *gnrhr1b* and *gnrhr2b* were performed as described previously (39) on 6-month old mature females from tg(*fshb*:DsRed2), tg(*lhb*:hrGfpII) or WT lines (see figure legends for details). First, we

146 investigated the % identity between the RNA probes and the target Gnrhr mRNA (Table 2),
147 and could observed that there were important sequence differences between a RNA probe and
148 the non-targeted *gnrhr* mRNA, thus making unlikely the possibility of unspecific cross
149 reaction Following, riboprobes were cloned into PCR-II TOPO (Thermo Fisher Scientific,
150 Massachusetts, USA) or PGEM-T Easy Vector (Promega, Wisconsin, USA) using primers
151 shown in Table 1 and cDNA from medaka brain and pituitary total RNA. After PCR with
152 M13 reverse and forward primers, sense and antisense probes were synthesized using SP6 or
153 T7 polymerase (Promega) and conjugated with either digoxygenin (DIG, Roche) or
154 fluorescein (FITC, Roche). The fish were euthanized with an overdose of tricaine (MS222;
155 Sigma-Aldrich, Missouri, USA) and tissues fixed by cardiac perfusion with 4%
156 paraformaldehyde (PFA; Electron Microscopy Sciences, Pennsylvania, USA). Free floating
157 60 μm parasagittal sections of brain and pituitary were made with a vibratome (VT1000S
158 Leica, Wetzlar, Germany). Tissue slices were incubated with hybridization probes for 18 h at
159 55ºC and then incubated with sheep anti-DIG and anti-FITC antibodies conjugated with
160 peroxidase (POD; 1:250; Roche) for probe labeling using the InSituPro VSI robot (Intavis,
161 Germany). Finally, the signal was revealed using custom made TAMRA-conjugated and
162 FITC-conjugated tyramides (39).
163
164 **Immunofluorescence**
165 Immunofluorescence (IF) was performed on free floating 60 μm parasagittal sections
166 as described previously (39). Briefly, brains and pituitaries from 6-month old tg(*gnrh1*:eGfp)
167 females were collected and fixed with 4% PFA. Tissues were then embedded in 3% agarose
168 before sectioning with a vibratome. Then, tissues were blocked for 1 h and incubated with
169 primary custom-made polyclonal rabbit anti-medakaLhβ (1:2000; AB_2732044) and anti-
170 medakaFshβ (1:500; AB_2732042), previously validated (40). For Fshβ IF, epitope retrieval

171 treatment using 2 N HCL (dissolved in phosphate buffered saline solution with 0.1% Tween,
172 PBST) for 1 h at 37ºC was necessary prior to blocking and antibody incubation. Signal was
173 amplified with secondary antibody AlexaFluor 555 (1:1000; AB_2535850 Invitrogen).
174 Sections were mounted in Vectashield Antifade Mounting Medium (Vector laboratories,
175 California, USA) and imaged as described below.
176
177 **DiI injection**
178 To label pituitary blood vessels, 6-month old siblings of the cross between
179 tg(*gnrh1*:eGfp) and tg(*fshb*:DsRed2), i.e. tg(*gnrh1*:eGfp/*fshb*:DsRed2), were euthanized with
180 an overdose of tricaine. Cardiac perfusion with DiIC18(5)-DS (1,1'-Dioctadecyl-3,3,3',3'-
181 Tetramethylindodicarbocyanine-5,5'-Disulfonic Acid; Thermo Fisher Scientific) diluted in
182 4% paraformaldehyde (PFA) was performed as described in (41).
183
184 **Confocal Imaging**
185 For whole pituitary imaging, pituitaries from tg(*gnrh1*:eGfp) females were collected,
186 fixed in 4% PFA and mounted between slide and coverslip with spacers in Vectashield
187 Antifade Mounting Medium. All confocal images were acquired using LSM710 confocal
188 microscope (Zeiss, Oberkochen, Germany) with 25X (N.A. 0.8) or 40X (N.A. 1.2) objectives.
189 Channels were acquired sequentially to avoid signal crossover between different filters.
190 Images were processed using ZEN software (version 2009, Zeiss). Z-projections from
191 confocal stacks of images were obtained using Fiji (version 2.0.0 (42)). 3D reconstruction
192 was built using Fiji 3D viewer plugin.
193
194 **Primary dispersed pituitary cell culture**

Pituitaries were collected from 10 mature, gravid females from the tg(*lhb*:hrGfpII) and tg(*fshb*:DsRed2) lines separately following decapitation and dissociated according to (43). In brief, pooled pituitaries were digested with trypsin (2 mg/mL, Sigma-Aldrich) for 30 min at 26ºC, then incubated with trypsin inhibitor (1 mg/mL, Sigma-Aldrich) and DNase I Type IV (2 µg/mL, Sigma-Aldrich) for 20 min at 26ºC with gentle shaking. Pituitary cells were mechanically dissociated using a glass pipette, centrifuged at 200 *g* and resuspended in growth medium (L-15, Life Technologies) adjusted to 280-290 mOsm with mannitol and to pH 7.75 with 10 mM $NaHCO_3$, 1.8 mM glucose, and penicillin/streptomycin (50 U/mL of medium, Lonza, Verviers, Belgium). Dissociated cells were plated on poly-L-lysine pre-coated dishes fitted with a central glass bottom (MatTek Corporation, Ashland, MA, USA). The cell density was low to prevent intercellular contact and cultures were used within 48 h after plating to minimize changes in gene expression. Three different cell cultures were made for patch clamping and for Ca^{2+} imaging. In each culture 2-7 primary target cells were stimulated by 1 µM Gnrh1 (Bachem Americas, Inc. CA, USA).

Live brain-pituitary slices

Using mature females from the tg(*lhb*:hrGfpII), tg(*fshb*:DsRed2), and tg(*lhb*:hrGfpII/*fshb*:DsRed2) lines, 150 µm brain-pituitary sections were made according to (44). In brief, following decapitation, the brain-pituitary complex was removed and embedded in 2% agarose (Sigma-Aldrich) dissolved in Ca^{2+}- and BSA-free Extracellular Solution (ECS) (mM): NaCl 134, KCl 2.9, $MgCl_2$ 1.2, HEPES 10, and glucose 4.5. The solution was adjusted to pH 7.75 with 1 M NaOH and osmolality adjusted to 290 mOsm with mannitol before filter sterilization. Following sectioning, the brain-pituitary slices were moved to the recording chamber containing ECS with 2 mM Ca^{2+} and 0.1% BSA.

220 **Electrophysiology**

221 All electrophysiological experiments were conducted using the perforated patch
222 clamp technique in current clamp on either brain-pituitary slices (44) or primary dissociated
223 cells (43) from the tg lines described above (*Live brain-pituitary slices*), and with ECS
224 containing 2 mM Ca^{2+} and 0.1% BSA. The experiments were conducted between 14:00 h and
225 19:00 h. Patch pipettes were made from thick-walled borosilicate glass with 4-5 MΩ
226 resistance. The following intracellular (IC) electrode solution was added to the patch pipette
227 (mM): KOH 120, KCl 20, HEPES 10, sucrose 20, EGTA 0.2. The pH was adjusted to 7.2
228 with $C_6H_{13}NO_4S$, and osmolality to 280 mOsm with sucrose. To perforate the cell membrane
229 amphotericin B (Sigma-Aldrich) was added to 0.24 mg/ml (see details in (44)). The electrode
230 was coupled to a Multiclamp 700B amplifier (Molecular Devices, California, USA). The
231 recorded signals were digitized at 4 to 10 kHz and filtered at one third of the sampling rate
232 using a Digidata 1550B plus with hum silencer (Molecular Devices). All commands and
233 recorded signals were handled using pClamp 10 software (Molecular Devices). Gnrh1
234 (Bachem) was dissolved to 1 µM in filtered ECS with 0.1% BSA and applied to brain-
235 pituitary slices or dispersed cells using 20 kPa puff ejection through a 2 MΩ pipette, 30-40
236 µm from the target cell. The cells were visualized using an Infrared Dot Gradient Contrast
237 (DGC) system coupled to an up-right microscope (Slicescope, Scientifica, Uckfield, UK)
238 with a 40X water immersion objective (N.A. 0.8, Olympus, Shinjuku, Japan). The genetically
239 labeled gonadotrope cells were visualized using a light-emitting diode light source (pE-4000
240 CoolLED, Andover, UK). DsRed2 was excited at 550 nm and emission collected after
241 passing a 630/75 nm bandpass filter (Chroma, Vermont, USA); hrGFPII was excited at 470
242 nm and emission was collected after passing a 525/50 nm bandpass filter (Chroma). Data
243 were analyzed using AxoGraph version X 1.7 (www.axograph.com) and Matlab version
244 R2018a (Mathworks, Massachusetts, USA).

245

246 **Microfluorimetry**

247 Ca^{2+} imaging on adult female pituitaries was performed separately for
248 tg(*fshb*:DsRed2) and tg(*lhb*:hrGfpII) using the calcium-indicator dyes Cal-590-AM (AAT
249 Bioquest, California, USA) for tg(*lhb*:hrGfpII), and Fluo4-AM (ThermoFisher Scientific,
250 Massachusetts, USA) for tg(*fshb*:DsRed2). Dyes were loaded at 5 µM 30 min (cell culture) or
251 60 min (brain-pituitary slices), at 27ºC in 2 mL BSA-free ECS with 1 µL 20% Pluronic
252 (Sigma), followed by 20 min in ECS with 0.1% BSA to de-esterify the dyes. Cal590 was
253 excited at 580 nm and emission images were collected following passage through a 630 nm
254 wavelength / 75 nm bandwidth filter (ET630/75 nm emitter, Chroma). Fluo4 was excited at
255 470 nm and emission images were collected following passage through a 525 nm wavelength
256 / 50 nm bandwidth filter (ET525/50 nm emitter, Chroma). Cells were imaged using a sCMOS
257 camera (optiMOS, QImaging, British Columbia, Canada) with 50 to 80 ms exposure and 1-2
258 Hz sampling frequency. Both light source and camera were controlled by µManger software,
259 version 1.4 (45). Relative fluorescence intensity was calculated after background subtraction
260 as changes in fluorescence (F) divided by the average intensity of the first 15 frames (F_0).
261 Data were analyzed using Fiji (46).

262

263 **Uncaging**

264 Uncaging experiments were performed on tg(*fshb*:DsRed2) and tg(*lhb*:hrGfpII), as
265 well as on the double tg(*lhb*:hrGfpII/*fshb*:DsRed2) line. In these experiments, 5 µM NP-
266 EGTA (caging compound) was loaded into the cells (same procedure as the dye loading
267 described above under Microfluorimetry) to chelate Ca^{2+}, followed by uncaging and
268 destruction of the NP-EGTA with 50-250 ms pulses from a 405 nm laser (Laser Applied
269 Stimulation and Uncaging system, Scientifica). The laser was pre-set at 7 mW and passed

through an 80/20 beam splitter before targeting the cells. The output effect was not calculated. The laser was guided and targeted at distinct regions of the cells using two galvanometer scan mirrors (one for each axis) controlled by Scientifica software developed in LabVIEW (National Instruments, Texas, USA). Laser reflection artifacts were removed post recording from the final imaging profile.

General figure making

Composites were assembled using Adobe Photoshop and Indesign CC (Adobe Inc, California, USA). Images were processed using ImageJ open source software (versions 1.37v and 2.0.0, National Institute of Health, USA). Photo montages were made in Adobe Photoshop, Adobe Illustrator, and Adobe Indesign CC2018 (Adobe Inc).

281 RESULTS

282 **Development of new medaka transgenic lines and mapping of gonadotrope cells in**
283 **medaka pituitary**

284 To study medaka Fsh cells, we developed a new transgenic line (tg(*fshb*:DsRed2)) in
285 which DsRed2 expression is controlled by the cloned 3833 bp endogenous *fshb* promotor.
286 Following confirmation of transgene homozygosity, specificity of the DsRed2 reporter was
287 verified using *in situ* hybridization. Multicolor fluorescent *in situ* hybridization with specific
288 probes for *fshb* and *dsred2* showed nearly complete co-localization of the two probes,
289 confirming that DsRed2 is a reliable marker for *fshb* cells in this line (Figure 1A-D). Fsh cells
290 were located in the median part of the *proximalis pars distalis* (PPD). Homozygous
291 tg(*fshb*:DsRed2) fish were crossed with the previously established tg(*lhb*:hrGfpII) line
292 (Figure 1E-H) established by Hildahl et al (36) and recently validated by Fontaine et al (47),
293 to obtain the double tg(*lhb*:hrGfpII/*fshb*:DsRed2). In the double tg line, the two cell types
294 expressing either *fshb* or *lhb* were clearly separated (Figure 1I-L). Fsh and Lh cells were
295 localized in the PPD, with Fsh cells in close proximity of the Lh cells. However, while Lh
296 cells were localized in the ventral and lateral part of the PPD, Fsh cells were localized more
297 medially.

298

299 **Localization of Gnrh1 fibers within the medaka pituitary**

300 To investigate the location of the hypophysiotropic Gnrh1 neuron fibers, we utilized
301 the established tg(*gnrh1*:eGfp) medaka (36). The majority of the PPD was well innervated by
302 Gnrh1 projections (Figure 2A and B), with most fibers reaching the ventral and lateral PPD
303 where Lh cells are located. Immunofluorescence to localize Fshβ (Figure 2C-F) and Lhβ
304 (Figure 2G-J) on tg(*gnrh1*:eGfp) pituitary slices showed that Gnrh1 projections were found in
305 the proximity of both gonadotrope cell types. In fact, Gnrh1 fibers project throughout the

306 whole PPD, passing next to Fsh cells and reaching the ventral and lateral surface, where Lh
307 cells are localized. Using fish perfused with DiI to visualize blood vessels we observed that
308 Gnrh1 projections also followed the path of the blood vessels. (Figure 2K and L).
309
310 **Expression of *gnrhr* in Fsh and Lh cells**
311 To further explore how Gnrh1 regulates Fsh and Lh we used qPCR to measure
312 transcripts of all four *gnrhr* paralogs identified in the medaka genome. While the four genes
313 were cloned from brain RNA, the qPCR assays revealed expression of only three receptor
314 genes in the pituitary (Figure 3A): *gnrhr1b*, *gnrhr2a* and *gnrhr2b*. Expression of *gnrhr2c* was
315 not detected in any of the pituitary samples. To identify cell specific expression, we used
316 double color fluorescent *in situ* hybridization combining each *gnrhr* with either *fshb* or *lhb*
317 (figure 3B-Z). *In situ* probes were designed to minimize the chances for cross reaction
318 between the probes and target *gnrhr* mRNA (Table 2). The results showed that *gnrh1b* is
319 expressed in the posterior part of the pituitary in some of the most posterior *lhb* cells but not
320 in *fshb* cells. *gnrhr2a* is expressed in the ventral surface of the pituitary, almost exclusively in
321 *lhb* cells and never in *fshb* cells. Indeed, a near full co-localization was observed with only a
322 few extra cells expressing *gnrhr2a* without *lhb*. Finally, *gnrhr2b* is expressed in the posterior
323 part of the pituitary, in a similar region to *gnrhr1b*, but was found in very few *lhb* cells (fewer
324 than for *gnrhr1b*), and never in *fshb* cells. Thus, using *in situ* hybridization, we found no
325 evidence of *gnrhr* expression in *fshb* cells.
326
327 **Effect of Gnrh1 on Fsh and Lh cells in dispersed pituitary cell culture**
328 To further explore and validate the *in situ* hybridization results we performed a series
329 of patch clamp and Ca^{2+} imaging experiments in which we stimulated dissociated medaka
330 pituitary cells with Gnrh1. These experiments were conducted 24-48 h after plating the cells.

During the initial current clamp recordings, we observed spontaneous firing of action potentials in 60% (n = 20) of the Fsh cells (Figure 4A), similar to our previous results on medaka Lh cells (21,22,43). The spontaneous firing of Fsh cells occurred in cells with oscillating membrane potential around -45 to -40 mV with the action potential often overshooting 0 mV (liquid junction potential not corrected for). The firing frequency of Fsh cells ranged from 0.5 to 3 Hz.

Consistent with the *in situ* hybridization results indicating that Lh cells express *gnrhr* whereas Fsh cells do not, we found a biphasic response (electrical and $[Ca^{2+}]_i$) to Gnrh1 in Lh cells (Figure 4B and C). The electrical response consisted of an initial membrane hyperpolarization followed by depolarization and a robust increase in action potential frequency (Figure 4B). This response reflects the changes in $[Ca^{2+}]_i$ with the initial membrane hyperpolarization being due to Ca^{2+} release from internal stores and subsequent activation of Ca^{2+} -activated K^+ channels. This initial release of Ca^{2+} from internal stores is followed by a plateau reflecting the influx of extracellular Ca^{2+} as a result of increased firing frequency (Figure 4D). In contrast to the biphasic response to Gnrh1 observed in Lh cells, we were not able to detect any changes (electrical or $[Ca^{2+}]_i$) in Fsh cells following Gnrh1 exposure (Figure 4A and C).

Effect of Gnrh1 on Fsh and Lh cells in live brain-pituitary tissue slices

To further investigate the results observed in cell culture, we utilized brain-pituitary tissue slices from the double tg(*lhb*:hrGfpII/*fshb*:DsRed2) line to separately target Fsh and Lh cells for electrophysiological experiments. In Fsh cells, we observed oscillatory spontaneous electrical activity (Figure 5A), with cells switching from a non-firing quiescent state to an excited state marked by burst-like sequences lasting 20-80 s.

355 Surprisingly, contrary to the results in dispersed cell cultures, about 60% of the Fsh
356 cells in the brain-pituitary slices responded to Gnrh1 (a total of 16 cells from 8 pituitaries)
357 (Figure 5B-F). All responding Fsh cells were located in close proximity to Lh cells. Both
358 electrical and increased $[Ca^{2+}]_i$ responses were either prolonged (i.e. lasting until the
359 recording ended after 4-6 minutes; Figure 5B, C, and E) or transient (i.e. lasting from 40 s up
360 to 5 minutes; Figure 5D and F) with a 1-5 s latency after addition of Gnrh1. The typical
361 electrical response to Gnrh1 was a membrane depolarization (Figure 5B). In non-firing Fsh
362 cells, the Gnrh1-induced depolarization was sufficient to initiate a prolonged burst. In some
363 cells we observed a weak hyperpolarization prior to depolarization (Figure 5C) without a
364 change in firing activity. In Fsh cells spontaneously generating action potentials, Gnrh1
365 caused a membrane depolarization and in a few cases led to broadening of the action
366 potential from 6-10 ms to over 20 ms. Some of the Fsh cells also responded to Gnrh1 with
367 small bursts (Figure 5D). The different Gnrh1-induced responses were never observed in
368 control experiments where we applied puff ejections of ECS onto cells. In fact, the electrical
369 activity could not be changed even when doubling the puff application pressure.

370 The electrophysiological responses of Lh cells in brain-pituitary slices to Gnrh1 were
371 similar to those observed in dissociated cell culture. We saw a clear electrical response in all
372 Lh cells following Gnrh1 stimulation with similar latency as in Fsh cells. In 9 out of 13 cells
373 (from 8 different pituitaries) we observed a biphasic response (Figure 6A). In the remaining 4
374 Lh cells (3 different pituitaries) out of the 13, we observed a monophasic response in which
375 Gnrh1 initiated a direct depolarization of the cell membrane (Figure 6B). This depolarization
376 was sufficient to initiate both transient and prolonged firing in previously quiescent cells. The
377 electrical responses were also reflected in the different Ca^{2+} responses to Gnrh1 (Figure 6C
378 and D). Prolonged and robust Ca^{2+} responses to Gnrh1 had two slightly different shapes. One
379 response was clearly biphasic similar to what we observed in cell culture, with an initial Ca^{2+}

peak (release of Ca^{2+} from internal stores) followed by a second phase plateau. The other Gnrh1-induced response was prolonged but lack the second plateau following. Following an initial peak, the Ca^{2+} levels gradually decreased but not to basal levels (Figure 6C). In a few cells, we could only detect a transient Ca^{2+} response lasting less than a minute (Figure 6D) before returning to baseline values.

Cell communication between gonadotrope cells in live brain-pituitary tissue slices

The divergent effects of Gnrh1 on Fsh cells in tissue slices and dissociated cell cultures, and the absence of detectable *gnrhr* mRNA in Fsh cells by FISH, led us to hypothesize that intercellular communication may mediate Gnrh1-induced excitation in Fsh cells. To test for intercellular electrical communication, we utilized Ca^{2+} uncaging in one gonadotrope cell and recorded changes in membrane potential in neighboring gonadotropes (Figure 7A). Uncaging of Ca^{2+} causes membrane hyperpolarization via activation of Ca^{2+}-activated K^+ channels (48). If there is direct electrical communication between two cells, altering the membrane potential in one cell should initiate changes in membrane potential in the other.

We observed that gonadotropes with soma-soma contact with an uncaged cell hyperpolarized within 15-20 ms of Ca^{2+} uncaging. We saw this rapid response in Fsh cell pairs (n = 11 cells from 3 different pituitaries) (Figure 7B) as well as Lh cell pairs (n = 13 from 3 different pituitaries) (Figure 7C) and more importantly, in Fsh-Lh cell pairs (n = 7 from 3 different pituitaries) (Figure 7D and E). This rapid propagation of the response is to the best of our knowledge too fast for the uncaged Ca^{2+} to diffuse from the target cell to the recorded cell and therefore points to direct electrical connection between the cells. Finally, to further explore intercellular communication, we tested whether Ca^{2+} uncaging could initiate $[Ca^{2+}]_i$ waves that reached surrounding cells. In fact, uncaging Ca^{2+} in Lh cells could generate

small waves that led to elevated $[Ca^{2+}]_i$ in all Lh cells tested (n = 9 target cells from 3 different pituitaries) (Figure 8A and B. Possible pathways illustrated in 8C). Typically, the Ca^{2+} signal only propagated to neighboring cells reaching maximum of 3 cells from the target cell. In contrast, following uncaging in Fsh cells, we were only able to see propagation of Ca^{2+} signal in 50% of the cells (n = 16 target cells from 3 pituitaries, data not shown).

DISCUSSION

In this study, we first show that the anatomical organization of the hypophysiotropic Gnrh (Gnrh1 in medaka) is similar to other teleost species (2-5). The Gnrh1 axons projects close to both Fsh and Lh cell as well as the pituitary blood vessels. Following, we find evidence that in female medaka, Gnrh1 stimulates Lh cells directly but Fsh cells indirectly, likely via interactions with directly activated Lh cells. This evidence is three-fold: 1) Fsh cells in female medaka lack expression of any of the three *gnrhr* paralogs present in the pituitary, whereas all Lh cells express at least one *gnrhr* paralog. 2) While Lh cells exhibited identical electrical and Ca^{2+} responses to Gnrh1 in dissociated pituitary cultures and in brain-pituitary tissue slices, Fsh cells showed no effect in dissociated pituitary cultures but did respond to Gnrh1 in brain-pituitary tissue slices. 3) Direct Lh cell activation rapidly induced electrical responses in neighboring Fsh cells. In addition, uncaging of Ca^{2+} in gonadotropes can initiate small $[Ca^{2+}]_i$ waves that propagate to surrounding cells.

Organization of gonadotrope cells and Gnrh1 fibers within the pituitary

To separately investigate Fsh and Lh cells we established a new tg line with expression of red fluorescent protein, Dsred2, controlled by the endogenous medaka *fshb* promoter. We confirm the specificity of *dsred2* in *fshb* cells with multicolor FISH. Moreover, Burow et al (40) reported that *fshb* cells also express Fshβ protein in the medaka pituitary.

Thus, we inferred that the *dsred2*-positive cells produce Fsh hormone and can therefore be referred to as Fsh cells. We then crossed tg(*fshb*:DsRed2) fish with fish from the previously established tg(*lhb*:hrGfpII) line (36,47) (Figure 1E-H) and examined the spatial distribution of Fsh and Lh cells. In agreement with prior studies in teleosts (7), in the double tg(*lhb*:hrGfpII/*fshb*:DsRed2) medaka Fsh and Lh were expressed by distinct pituitary cells, thereby validating its use to simultaneously study Fsh and Lh cells (Figure1I-L).

Lh cells were found to be clustered in the ventral and lateral surface of the pituitary, whereas Fsh cells appeared more spread out and generally located more dorsally than Lh cells. However, Fsh cells were often found in close proximity, and in some cases appeared in direct contact, with other Fsh cells. Significantly, Fsh cells also appeared to make direct contact with Lh cells along the ventral line of the pituitary. Similar observations have been made in zebrafish (*Danio rerio*) where Fsh cells were found at the periphery of Lh-cell clusters (49).

Similar to that reported for other fish species (2-5), we found that Gnrh1 neurons directly innervate the pituitary in female medaka. Gnrh1 projections were seen throughout the PPD where both Fsh and Lh cells are located, and alongside blood vessels (Figure 2A -J). This organization is quite similar to that of Gnrh3 neurons in zebrafish (5). We did not see projections terminating directly on gonadotrope cells, and therefore cannot determine if Fsh and Lh cells are directly targeted. Golan et al (5) reported that Gnrh3 neurons innervating the pituitary in adult zebrafish had varicosity-like structures or boutons. In female medaka, we could not find such structures, but because we did not label the Gnrh1 neurons with synaptic markers, we cannot rule out their existence. We did detect small blebs in close contact with blood vessels (Figure 2K and L). However, during pituitary sectioning, the orientation of blood vessels and Gnrh1 neurons relative to the direction of the cut may introduce bouton-

like artifacts in transversally cut neurons. Therefore, additional studies are needed to clarify the exact morphology of the Gnrh1 projections and the precise location of the terminals.

Lh cells express *gnrhr*, but Fsh cells do not

Four *gnrhr* paralogs have been identified in the medaka genome and expressed in the adult medaka brain (50). In a previous study, two of the *gnrhr* paralogs were found to be expressed in the adult female medaka pituitary, namely *gnrhr1b* and *gnrhr2a* (21). In the present study, we detected one additional paralog; *gnrhr2b*. Expression of multiple *gnrhr* paralogs in the pituitary has been observed in other teleost species including goldfish (*Carassius auratus*)(51), tilapia (*Oreochromis niloticus*)(28,52) and (*Astatotilapia burtoni*)(53), and Atlantic cod (*Gadus morhua*)(54). Using *in situ* hybridization on brain-pituitary slices from female medaka, we found *gnrhr* expressed in the median and posterior part of the pituitary. While *gnrhr1b* and *gnrhr2b* were expressed in the PI, only *gnrhr2a* was expressed in the PPD, and almost exclusively in Lh cells (Figure 3). These results support a previous study where *gnrhr2a* was the paralog showing the highest expression levels in the pituitary of both juvenile and adult medaka (50). The same study revealed that *gnrhr2a* expression levels increased in parallel with the number of pituitary Lh cells between juvenile and adult fish (50).

Interestingly, *lhb* cells from Atlantic cod were found to express *gnrhr1b* and *gnrhr2a* (54). More recently, a novel *gnrhr*, *gnrhr2baα*, was found in *lhb* cells from Atlantic salmon (29). It is interesting to note that the *gnrhr* identified in Lh cells from Atlantic salmon, Atlantic cod, and medaka belong to the same phylogenetic group, suggesting they share a common ancestral gene (29).

To our surprise, we did not co-localize any *gnrhr* with *fshb*. This contradicts previous reports of *gnrhr* expression in *fshb* cells from Atlantic cod (19,54) and tilapia (28). This

479 disparity may be due to species or sex differences, or to differences in methodology. The
480 work in Atlantic cod was performed on primary dissociated pituitary cells pooled from both
481 sexes and conducted at 2 to 7 days after plating (19,54). This difference in timing may be
482 important, as a previous study found that *gnrhr* expression increased in pituitary cell culture
483 over time (55), suggesting that either *gnrhr* expression increases in cells already expressing
484 the receptor or that new cells start to express *gnrhr*. In tilapia, single-cell PCR found
485 measurable *gnrhr* transcripts in *fshb* cells in fixed tissue; however, this study only analyzed
486 pituitaries from males (28). Therefore, further studies are needed to clarify whether *gnrhr*
487 expression patterns vary among species or between sexes. Notably, the expression pattern we
488 report for female medaka is similar to that observed during embryogenesis in mouse, where
489 FSH and LH are produced in distinct cells within the pituitary and during this time GnRHR
490 are expressed exclusively in LH cells and not in FSH cells (56).
491
492 **Effects of Gnrh1 on Fsh and Lh cells in cell culture**
493 In the present study both the electrophysiological recordings and Ca^{2+} changes in
494 cultured cells treated with Gnrh1 are consistent with the *in situ* hybridization results. We
495 found that female medaka Lh cells clearly responded to Gnrh1, inducing elevated $[Ca^{2+}]_i$ and
496 altered electrophysiological behavior. Conversely, we did not detect changes in membrane
497 potential or Ca^{2+} levels in Fsh cells upon exposure to Gnrh1 up to 48 h after plating the
498 dispersed pituitary cells. These results confirm that the *in situ* hybridization is adequately
499 sensitive and all together suggest that unlike Lh cells, adult female medaka Fsh cells do not
500 express *gnrhr*.
501 The response of Lh cells to Gnrh1 is consistent with that previously reported for other
502 teleosts (19,21,22,43). However, very few studies have examined electrical activity or
503 calcium flux of cultured teleost Fsh cells in response to Gnrh1. In dispersed Atlantic cod

pituitary cultures, Gnrh increased action potential frequency and $[Ca^{2+}]_i$ in Fsh cells, suggesting that Fsh cells possess functional Gnrhr (19). However, as noted above, that study was conducted after the dispersed pituitary cells had been maintained for 2 to 7 days in culture, which may have induced phenotypic changes such as altered *gnrhr* expression. As a result of these contradictory results, a more systematic testing of Gnrh induced responses using primary pituitary cells should be conducted to reveal if gonadotrope cells alter their Gnrhr composition with time in culture.

Effects of Gnrh1 on Fsh and Lh cells in brain-pituitary tissue slices

Both Fsh and Lh cells fired spontaneous action potentials in brain-pituitary slices (Figure 5 and 6). In addition, long current clamp recordings of Fsh cells demonstrated membrane potential oscillations, with quiescent periods followed by weak depolarization and subsequent firing of action potentials. These longer bursts of spontaneous action potentials could mediate basal release of Fsh, but further experiments are needed to resolve their exact role. Using inverse-Pericam transgenic medaka, Karigo et al (20) observed that unstimulated Lh cells exhibited regular synchronized $[Ca^{2+}]_i$ oscillations. Fsh cells had more desynchronized $[Ca^{2+}]_i$ oscillations with lower peaks compared to Lh cells. However, the frequency of $[Ca^{2+}]_i$ peaks were higher in Fsh cells. Importantly, the $[Ca^{2+}]_i$ oscillations were demonstrated to be independent of Gnrh (20).

Surprisingly, despite finding no expression of *gnrhr* in Fsh cells, and no response to Gnrh1 in dissociated Fsh cells, Fsh cells in brain-pituitary slices did respond to Gnrh1 (Figure 5). This result agrees with findings reported by Karigo et al (20) who showed that Gnrh1 elicited elevated $[Ca^{2+}]_i$ levels in Fsh cells in whole brain-pituitary preparations from female medaka (20). Furthermore, this is the first clear demonstration that the effects of Gnrh1 on Fsh cells are indirect.

529

530 **Cellular communication between gonadotrope cells**

531 Because Fsh cells respond to Gnrh1 in tissue slice preparations but not in dispersed
532 cell cultures, and because they lack functional Gnrh receptors, we explored the possibility of
533 communication between gonadotrope cells in pituitary slices (Figure 8). By using Ca^{2+}
534 uncaging and patch clamping on genetically labeled Fsh and Lh cells, we separately targeted
535 the cells within the same preparation. Indeed, current clamp recordings demonstrated that not
536 only is homotypic communication between Fsh cells or between Lh cells possible, but Fsh
537 and Lh cells form heterotypic networks as well. Such cell-cell networks allow rapid electrical
538 communication, whereby information received by one cell can be quickly relayed to several
539 cells. Coupling of cells in the pituitary has been shown to greatly affect hormone release in
540 both mammals and teleost fish (33,34,57,58). However, blocking gap junctions responsible
541 for cytosolic bridging between cells had less impact on Gnrh induced Fsh release than Lh
542 release in tilapia (34). This observation is consistent with our finding that the responses of
543 Fsh cells to Gnrh1 were weaker than that of Lh cells. In fact, as previously reported, normal
544 folliculogenesis is seen in Gnrh knockout medaka (13). In addition, in mammals only a 50%
545 reduction in plasma FSH is observed in GnRH deficient *hpg* mouse (30). These results
546 suggest that FSH is more dependent on other factors than GnRH. Therefore, additional
547 investigations are required to identify all factors responsible in the differential regulation of
548 Fsh and Lh.

549 In our experiments we clearly see that Ca^{2+} uncaging in single cells can propagate
550 between Lh cells (Figure 8) which may explain the synchronicity of the Ca^{2+} flux in Lh cells
551 observed by Karigo et al (20). Future studies combining uncaging with Ca^{2+} imaging could
552 reveal potential differences between Fsh and Lh cells in how Ca^{2+} propagates between the
553 cells.

554 To conclude, we provide evidence that while Lh cells in female medaka respond
555 directly to Gnrh1, Fsh cells do not. However, Fsh cells can respond to Gnrh1 when they are
556 associated with other pituitary cells. We also provide evidence of electrical signaling among
557 gonadotropes. We propose that such signaling may play an important role in gonadotrope
558 physiology and suggest that intercellular electrical signaling may mediate hormone release
559 and permit Fsh cell response to Gnrh1.

560 References

561

562 1. Knigge KM, Scott DE. Structure and function of the median eminence. *Am J Anat*.
563 1970;129(2):223-243.

564 2. Ball JN. Hypothalamic control of the pars distalis in fishes, amphibians, and reptiles.
565 *Gen Comp Endocrinol*. 1981;44(2):135-170.

566 3. Knowles F, Vollrath L. Synaptic contacts between neurosecretory fibres and
567 pituicytes in the pituitary of the eel. *Nature*. 1965;206(4989):1168-1169.

568 4. Knowles F, Vollrath L. Neurosecretory innervation of the pituitary of the eels
569 *Anguilla* and *Conger* I. The structure and ultrastructure of the neuro-intermediate lobe
570 under normal and experimental conditions. *Phil Trans R Soc Lond B*.
571 1966;250(768):311-327.

572 5. Golan M, Zelinger E, Zohar Y, Levavi-Sivan B. Architecture of GnRH-Gonadotrope-
573 Vasculature Reveals a Dual Mode of Gonadotropin Regulation in Fish.
574 *Endocrinology*. 2015;156(11):4163-4173.

575 6. Childs GV. Cytochemical studies of multifunctional gonadotropes. *Microsc Res Tech*.
576 1997;39(2):114-130.

577 7. Kanda S, Okubo K, Oka Y. Differential regulation of the luteinizing hormone genes
578 in teleosts and tetrapods due to their distinct genomic environments--insights into
579 gonadotropin beta subunit evolution. *Gen Comp Endocrinol*. 2011;173(2):253-258.

580 8. Weltzien FA, Hildahl J, Hodne K, Okubo K, Haug TM. Embryonic development of
581 gonadotrope cells and gonadotropic hormones--lessons from model fish. *Mol Cell*
582 *Endocrinol*. 2014;385(1-2):18-27.

583 9. Nozaki M, Naito N, Swanson P, Miyata K, Nakai Y, Oota Y, Suzuki K, Kawauchi H.
584 Salmonid pituitary gonadotrophs. I. Distinct cellular distributions of two
585 gonadotropins, GTH I and GTH II. *Gen Comp Endocrinol*. 1990;77(3):348-357.
586 10. Schmitz M, Aroua S, Vidal B, Le Belle N, Elie P, Dufour S. Differential regulation of
587 luteinizing hormone and follicle-stimulating hormone expression during ovarian
588 development and under sexual steroid feedback in the European eel.
589 *Neuroendocrinology*. 2005;81(2):107-119.
590 11. Gharib SD, Wierman ME, Shupnik MA, Chin WW. Molecular biology of the
591 pituitary gonadotropins. *Endocr Rev*. 1990;11(1):177-199.
592 12. Schulz RW, Vischer HF, Cavaco JE, Santos EM, Tyler CR, Goos HJ, Bogerd J.
593 Gonadotropins, their receptors, and the regulation of testicular functions in fish. *Comp*
594 *Biochem Physiol B Biochem Mol Biol.* 2001;129(2-3):407-417.
595 13. Takahashi A, Kanda S, Abe T, Oka Y. Evolution of the hypothalamic-pituitary-
596 gonadal axis regulation in vertebrates revealed by knockout medaka. *Endocrinology*.
597 2016;157(10):3994-4002.
598 14. Swanson P, Dickey JT, Campbell B. Biochemistry and physiology of fish
599 gonadotropins. *Fish Physiol Biochem.* 2003;28(1-4):53-59.
600 15. Levavi-Sivan B, Bogerd J, Mananos EL, Gomez A, Lareyre JJ. Perspectives on fish
601 gonadotropins and their receptors. *Gen Comp Endocrinol*. 2010;165(3):412-437.
602 16. Burger LL, Dalkin AC, Aylor KW, Haisenleder DJ, Marshall JC. GnRH pulse
603 frequency modulation of gonadotropin subunit gene transcription in normal
604 gonadotropes-assessment by primary transcript assay provides evidence for roles of
605 GnRH and follistatin. *Endocrinology*. 2002;143(9):3243-3249.

606 17. Dalkin AC, Haisenleder DJ, Ortolano GA, Ellis TR, Marshall JC. The frequency of
607 gonadotropin-releasing-hormone stimulation differentially regulates gonadotropin
608 subunit messenger ribonucleic acid expression. *Endocrinology*. 1989;125(2):917-924.
609 18. Haisenleder DJ, Dalkin AC, Ortolano GA, Marshall JC, Shupnik MA. A pulsatile
610 gonadotropin-releasing hormone stimulus is required to increase transcription of the
611 gonadotropin subunit genes: evidence for differential regulation of transcription by
612 pulse frequency in vivo. *Endocrinology*. 1991;128(1):509-517.
613 19. Hodne K, Strandabo RA, von Krogh K, Nourizadeh-Lillabadi R, Sand O, Weltzien
614 FA, Haug TM. Electrophysiological differences between *fshb*- and *lhb*-expressing
615 gonadotropes in primary culture. *Endocrinology*. 2013;154(9):3319-3330.
616 20. Karigo T, Aikawa M, Kondo C, Abe H, Kanda S, Oka Y. Whole brain-pituitary in
617 vitro preparation of the transgenic medaka (*Oryzias latipes*) as a tool for analyzing the
618 differential regulatory mechanisms of LH and FSH release. *Endocrinology*.
619 2014;155(2):536-547.
620 21. Strandabo RA, Gronlien HK, Ager-Wick E, Nourizadeh-Lillabadi R, Hildahl JP,
621 Weltzien FA, Haug TM. Identified lhb-expressing cells from medaka (*Oryzias*
622 *latipes*) show similar Ca^{2+}-response to all endogenous Gnrh forms, and reveal
623 expression of a novel fourth Gnrh receptor. *Gen Comp Endocrinol*. 2016;229:19-31.
624 22. Strandabo RA, Hodne K, Ager-Wick E, Sand O, Weltzien FA, Haug TM. Signal
625 transduction involved in GnRH2-stimulation of identified LH-producing
626 gonadotropes from lhb-GFP transgenic medaka (*Oryzias latipes*). *Mol Cell*
627 *Endocrinol*. 2013;372(1-2):128-139.
628 23. Ando H, Swanson P, Kitani T, Koide N, Okada H, Ueda H, Urano A. Synergistic
629 effects of salmon gonadotropin-releasing hormone and estradiol-17β on gonadotropin

subunit gene expression and release in masu salmon pituitary cells in vitro. *Gen Comp Endocrinol* 2004;137(1):109-121.

24. Dickey JT, Swanson P. Effects of salmon gonadotropin-releasing hormone on follicle stimulating hormone secretion and subunit gene expression in coho salmon (*Oncorhynchus kisutch*). *Gen Comp Endocrinol.* 2000;118(3):436-449.

25. Yaron Z, Gur G, Melamed P, Rosenfeld H, Elizur A, Levavi-Sivan B. Regulation of fish gonadotropins. *Int Rev Cytol*. 2003;225:131-185.

26. Ikemoto T, Park M. Identification and molecular characterization of three GnRH ligands and five GnRH receptors in the spotted green pufferfish. *Mol cell endocrinol*. 2005;242(1-2):67-79.

27. Moncaut N, Somoza G, Power DM, Canário AV. Five gonadotrophin-releasing hormone receptors in a teleost fish: isolation, tissue distribution and phylogenetic relationships. *J mol endocrinol.* 2005;34(3):767-779.

28. Parhar IS, Ogawa S, Sakuma Y. Three GnRH receptor types in laser-captured single cells of the cichlid pituitary display cellular and functional heterogeneity. *Proc Natl Acad Sci U S A*. 2005;102(6):2204-2209.

29. Ciani E, Fontaine R, Maugars G, Nourizadeh-Lillabadi R, Andersson E, Bogerd J, von Krogh K, Weltzien FA. Expression of Gnrh receptor gnrhr2bba exclusively in lhb-expressing cells in Atlantic salmon male parr. 2019; *Gen Comp Endocrinol*. *Submitted.*

30. Tsutsumi R, Webster NJ. GnRH pulsatility, the pituitary response and reproductive dysfunction. *Endocrine journal*. 2009;56(6):729-737.

31. Cattanach BM, Iddon CA, Charlton HM, Chiappa SA, Fink G. Gonadotrophin-releasing hormone deficiency in a mutant mouse with hypogonadism. *Nature*. 1977;269(5626):338-340.

32. Duran-Pasten ML, Fiordelisio T. GnRH-induced Ca^{2+} signaling patterns and gonadotropin secretion in pituitary gonadotrophs. Functional adaptations to both ordinary and extraordinary physiological demands. *Front Endocrinol (Lausanne)*. 2013;4:127.

33. Göngrich C, García-González D, Le Magueresse C, Roth LC, Watanabe Y, Burks DJ, Grinevich V, Monyer H. Electrotonic coupling in the pituitary supports the hypothalamic-pituitary-gonadal axis in a sex specific manner. *Front mol neurosci*. 2016;9:65.

34. Golan M, Martin AO, Mollard P, Levavi-Sivan B. Anatomical and functional gonadotrope networks in the teleost pituitary. *Sci Rep*. 2016;6:23777.

35. Takahashi A, Islam MS, Abe H, Okubo K, Akazome Y, Kaneko T, Hioki H, Oka Y. Morphological analysis of the early development of telencephalic and diencephalic gonadotropin□releasing hormone neuronal systems in enhanced green fluorescent protein□expressing transgenic medaka lines. *J Comp Neurol*. 2016;524(4):896-913.

36. Hildahl J, Sandvik GK, Lifjeld R, Hodne K, Nagahama Y, Haug TM, Okubo K, Weltzien FA. Developmental tracing of luteinizing hormone beta-subunit gene expression using green fluorescent protein transgenic medaka (*Oryzias latipes*) reveals a putative novel developmental function. *Dev Dyn*. 2012;241(11):1665-1677.

37. Weltzien FA, Pasqualini C, Vernier P, Dufour S. A quantitative real-time RT-PCR assay for European eel tyrosine hydroxylase. *Gen Comp Endocrinol*. 2005;142(1-2):134-142.

38. Kim M, Gee M, Loh A, Rachatasumrit N. Ref-finder: a refactoring reconstruction tool based on logic query templates. In: Press A, ed. Proceedings of the Eighteenth ACM SIGSOFT International Symposium on Foundations of Software engineering, ser. FSE ’10. New York. 2010:371-372.

680 39. Fontaine R, Affaticati P, Yamamoto K, Jolly C, Bureau C, Baloche S, Gonnet F,
681 Vernier P, Dufour S, Pasqualini C. Dopamine inhibits reproduction in female
682 zebrafish (*Danio rerio*) via three pituitary D2 receptor subtypes. *Endocrinology*.
683 2013;154(2):807-818.
684 40. Burow S, Fontaine R, Von Krogh K, Mayer I, Nourizadeh-Lillabadi R, Hollander-
685 Cohen L, Cohen Y, Shpilman M, Levavi-Sivan B, Weltzien FA. Medaka Follicle-
686 stimulating hormone (Fsh) and Luteinizing hormone (Lh): Developmental profiles of
687 pituitary protein and gene expression levels. *Gen Comp Endocrinol*. 2019;272:93-
688 108.
689 41. Fontaine R, Weltzien FA. Labeling of blood vessels in the teleost brain and pituitary
690 using cardiac perfusion with a DiI-fixative. *J Vis Exp*. 2019;(148):e59768.
691 42. Schindelin J, Arganda-Carreras I, Frise E, Kaynig V, Longair M, Pietzsch T,
692 Preibisch S, Rueden C, Saalfeld S, Schmid B, Tinevez JY, White DJ, Hartenstein V,
693 Eliceiri K, Tomancak P, Cardona A. Fiji: an open-source platform for biological-
694 image analysis. *Nat Methods*. 2012;9(7):676-682.
695 43. Ager-Wick E, Hodne K, Fontaine R, von Krogh K, Haug TM, Weltzien FA.
696 Preparation of a high-quality primary cell culture from fish pituitaries. *J Vis Exp*.
697 2018;(138):e58159.
698 44. Fontaine R, Hodne K, Weltzien FA. Healthy brain-pituitary slices for
699 electrophysiological investigations of pituitary cells in teleost fish. *J Vis Exp*.
700 2018(138):e57790.
701 45. Edelstein AD, Tsuchida MA, Amodaj N, Pinkard H, Vale RD, Stuurman N.
702 Advanced methods of microscope control using μManager software. *J Biol Methods*.
703 2014;1(2).

704 46. Schindelin J, Arganda-Carreras I, Frise E, Kaynig V, Longair M, Pietzsch T,
705 Preibisch S, Rueden C, Saalfeld S, Schmid B, Tinevez J-Y, White DJ, Hartenstein V,
706 Eliceiri K, Tomancak P, Cardona A. Fiji: an open-source platform for biological-
707 image analysis. *Nat Methods*. 2012;9(7):676-682.
708 47. Fontaine R, Ager-Wick E, Hodne K, Weltzien FA. Plasticity of Lh cells caused by
709 cell proliferation and recruitment of existing cells. *J Endocrinol*. 2019;240(2):361-
710 377.
711 48. Halnes G, Haug TM, Einevoll G, Weltzien FA, Hodne K. A computational model for
712 gonadotropin releasing cells in the teleost fish medaka. *PLOS Comput Biol*.
713 2019;accepted.
714 49. Golan M, Biran J, Levavi-Sivan B. A novel model for development, organization, and
715 function of gonadotropes in fish pituitary. *Front Endocrinol (Lausanne)*. 2014;5:182.
716 50. Strandabø RA, Grønlien HK, Ager-Wick E, Nourizadeh-Lillabadi R, Hildahl JP,
717 Weltzien F-A, Haug TM. Identified *lhb*-expressing cells from medaka (*Oryzias*
718 *latipes*) show similar Ca^{2+}-response to all endogenous Gnrh forms, and reveal
719 expression of a novel fourth Gnrh receptor. *Gen comp endocrinol*. 2016;229:19-31.
720 51. Illing N, Troskie BE, Nahorniak CS, Hapgood JP, Peter RE, Millar RP. Two
721 gonadotropin-releasing hormone receptor subtypes with distinct ligand selectivity and
722 differential distribution in brain and pituitary in the goldfish (*Carassius auratus*).
723 *Proc Natl Acad Sci U S A*. 1999;96(5):2526-2531.
724 52. Parhar IS, Soga T, Sakuma Y, Millar RP. Spatio-temporal expression of
725 gonadotropin-releasing hormone receptor subtypes in gonadotropes, somatotropes and
726 lactotropes in the cichlid fish. *J Neuroendocrinol*. 2002;14(8):657-665.
727 53. Flanagan CA, Chen C-C, Coetsee M, Mamputha S, Whitlock KE, Bredenkamp N,
728 Grosenick L, Fernald RD, Illing N. Expression, structure, function, and evolution of

gonadotropin-releasing hormone (GnRH) receptors GnRH-R1 SHS and GnRH-R2 PEY in the teleost, *Astatotilapia burtoni*. *Endocrinology*. 2007;148(10):5060-5071.

54. von Krogh K, Bjorndal GT, Nourizadeh-Lillabadi R, Hodne K, Ropstad E, Haug TM, Weltzien FA. Sex steroids differentially regulate *fshb*, *lhb* and *gnrhr* expression in Atlantic cod (*Gadus morhua*). *Reproduction*. 2017;154(5):581-594.

55. Hodne K, von Krogh K, Weltzien FA, Sand O, Haug TM. Optimized conditions for primary culture of pituitary cells from the Atlantic cod (*Gadus morhua*). The importance of osmolality, pCO_2, and pH. *Gen Comp Endocrinol*. 2012;178(2):206-215.

56. Wen S, Ai W, Alim Z, Boehm U. Embryonic gonadotropin-releasing hormone signaling is necessary for maturation of the male reproductive axis. *Proc Natl Acad Sci U S A*. 2010;107(37):16372-16377

57. Morand I, Fonlupt P, Guerrier A, Trouillas J, Calle A, Remy C, Rousset B, Munari-Silem Y. Cell-to-cell communication in the anterior pituitary: evidence for gap junction-mediated exchanges between endocrine cells and folliculostellate cells. *Endocrinology*. 1996;137(8):3356-3367.

58. Hodson DJ, Romanò N, Schaeffer M, Fontanaud P, Lafont C, Fiordelisio T, Mollard P. Coordination of calcium signals by pituitary endocrine cells in situ. *Cell calcium*. 2012;51(3-4):222-230.

750 **Table 1:** Genes, primers and accession numbers for cloning experiments.

751

752 **Table 2:** Percent sequence identity between *gnrhr* RNA probes and the mRNA for the

753 different *gnrhr* paralogs in medaka.

754

755

756 FIGURE LEGENDS

757

758 **Figure 1: Confirmation of the Fshβ and Lhβ reporter gene expression and generation of**
759 **the double transgenic line**. (A-D) Confocal images of parasagittal sections of medaka brain
760 and pituitary from the *fshb*-DsRed2 transgenic line, (E-H) the *lhb*-hrGfpII transgenic line, or
761 (I-L) the double transgenic line. (A-D) Tissue sections were labeled for *fshb* and *dsred2* by
762 FISH. (E-H) Tissue sections were labeled for *lhb* by FISH. (D), (H) and (L), represent the
763 merged images from the respective left panels together with nuclear (DAPI) staining.
764 Anterior to the left and dorsal to the top. Scale bars: 20 µm.

765

766 **Figure 2: Pituitary innervation by genetically labeled Gnrh1 neurons.** (A-B) Z-
767 projections of confocal images from the whole pituitary without (A) or with nuclear (DAPI)
768 staining (B) from the tg(*gnrh1*-eGfp) line. Anterior to the top. (C-J) Confocal images of
769 parasagittal brain-pituitary sections from the tg(*gnrh1*-eGfp) labeled for Fshβ (C-I) or Lhβ
770 (G-J) by IF. (F) and (J) represent the merged images from the respective left panels together
771 with nuclear (DAPI) staining. (K-H) Z-projections (5 µm z-stack) from confocal images of
772 parasagittal brain-pituitary sections from the siblings of the cross between tg(*gnrh1*-eGfp)
773 and tg(*fshb*-DsRed2), i.e. tg(*gnrh1*-eGfp/*fshb*-DsRed2), cardiac perfused with DiI. Scale bars:
774 20 µm.

775

776 **Figure 3: *gnrh* receptor (*gnrhr*) expression in the pituitary**. (A) Graphic presenting the
777 relative expression (mean + SEM) of the four *gnrhr* paralogs in both male and female
778 medaka pituitary. (B) Schema presenting the area of expression of the three *gnrhr* expressed
779 in the pituitary and the location of the Fsh and Lh cells therefore summarizing the

780 observations in the remaining panels. (C-Z) Confocal images of brain-pituitary parasagittal
781 sections double-labelled by FISH for *gnrhr1b* together with *fshb* (C-F) or *lhb* (G-J), *gnrhr2a*
782 together with *fshb* (K-N) or *lhb* (O-R) or *gnrhr2b* together with *fshb* (S-V) or *lhb* (W-Z). (F),
783 (J), (N), (R) and (V) represent the merged images from the respective left panels together
784 with nuclear (DAPI) staining. Anterior to the left and dorsal to the top. Scale bars: 50 μm.
785
786 **Figure 4: Gnrh1-induced electrical and Ca^{2+} responses of Fsh and Lh cells from**
787 **primary dispersed cell cultures**. The experiments were conducted in dispersed pituitary
788 cells from adult female medaka, using tg(*lhb*:hrGfpII/*fshb*:DsRed2) for electrophysiology and
789 tg(*lhb*:hrGfpII) or (*fshb*:DsRed2) for Ca^{2+} imaging. (A) Typical current clamp recording of a
790 spontaneously firing Fsh cell. Following Gnrh1 application (orange transparent bar
791 overlaying the trace), no apparent changes in the electrical response could be observed (a
792 total of n = 8 cells from 3 different cell cultures combined). (B) Typical current clamp
793 recording of a spontaneously firing Lh cell. Gnrh1 application using puff ejections induced a
794 biphasic response with an initial hyperpolarization followed by depolarization and increased
795 firing and/or increase action potential duration (see also (43)). (C) Ca^{2+} imaging of an Fsh
796 cell. Following Gnrh1 application no response was observed in Fsh cells (a total of n = 10
797 cells from 3 different cell cultures combined). (D) Gnrh1-induced Ca^{2+} response of an Lh
798 cell. The Lh cells responded to Gnrh1 with a biphasic increase in $[Ca^{2+}]_i$ mirroring the
799 electrical response in (A) (see details in (21,22)).
800
801 **Figure 5: Basal action potential firing properties and Gnrh1-induced responses of Fsh**
802 **cells in brain-pituitary slices**. The experiments were conducted using adult female medaka,
803 tg(*lhb*:hrGfpII/*fshb*:DsRed2) for electrophysiology and tg(*fshb*:DsRed2) for Ca^{2+} imaging.
804 (A) Prolonged current clamp recording of a spontaneous firing Fsh cell. The Fsh cells had

oscillatory firing properties where episodes of silence were followed by bursts of action potentials lasting 20-80 s. (B-D) Three types of electrical responses were observed in Fsh cells following Gnrh1 stimulation. (B) Current clamp recording of a non-firing Fsh cell. Gnrh1 application (orange transparent bar overlaying the trace) induced a monophasic response with membrane depolarization to threshold inducing action potentials. (C) Current clamp recording of a spontaneous firing Fsh cell. Gnrh1 elicited a weak biphasic response with an initial hyperpolarization but without any interruption in action potential pattern. The weak hyperpolarization was followed by a weak depolarization and increased action potential duration. (D) Current clamp recording of a spontaneous firing Fsh cell. Gnrh1 elicited a transient increase in firing frequency from 0.5-1 Hz to 2-3 Hz lasting 20-50 s. Two types of Ca^{2+} responses were observed in Fsh cells, prolonged and transient following Gnrh1 stimulation (E and F). (E) Ca^{2+} imaging of an Fsh cell stimulated by Gnrh1. The Fsh cells responded to Gnrh1 with increased $[Ca^{2+}]_i$ with an initial peak followed by a gradual decline. The responses usually lasted more than 60 s. (F) Transient Ca^{2+} response to Gnrh1 was also observed in Fsh cells, lasting 20-50 s.

Figure 6: Gnrh1-induced electrical and Ca^{2+} responses of Lh cells in brain-pituitary slices. The experiments were conducted using adult female medaka, tg(*lhb*:hrGfpII/*fshb*:DsRed2) for electrophysiology and the tg(*lhb*:hrGfpII) for Ca^{2+} imaging. Two types of Gnrh1-induced responses could be observed in Lh cells. (A) Typical current clamp recording of a spontaneous firing Lh cell. Gnrh1 stimulation (orange transparent bar overlaying the trace) induced a biphasic response with an initial hyperpolarization followed by a depolarization and increased firing and/or increase action potential duration. (B) Current clamp recording of a quiescent Lh cell. Gnrh1 elicited a monophasic response with a depolarization of the cell membrane to threshold, inducing action potentials. (C)

Ca^{2+} responses of an Lh cell stimulated by Gnrh1. The Lh cells responded to Gnrh1 with either a biphasic increase in $[Ca^{2+}]_i$ mirroring the electrical response in (A) or a prolonged response with an initial $[Ca^{2+}]_i$ peak followed by a gradual decrease. The responses usually lasted more than 60 s. (D) A few Lh cells responded to Gnrh1 with a transient elevation in $[Ca^{2+}]_i$ lasting 20-50 s.

Figure 7: Electrophysiological responses to uncaging of Ca^{2+} in neighboring gonadotrope cells. The experiments were conducted using adult female tg(*lhb*:hrGfpII/*fshb*:DsRed2). (A) A schematic overview of the experimental procedure of simultaneous uncaging and current clamp (voltage) recordings performed on gonadotrope cells from brain-pituitary slices. (B-E) Recording of the electrophysiological response in different gonadotrope cells following uncaging in neighboring cell. (B) Voltage recording of an Fsh cell, uncaging in neighboring Fsh cell. (C) Voltage recording of an Lh cell and uncaging in neighboring Lh cell. (D) Voltage recording of an Lh cell and uncaging in neighboring Fsh cell. (E) Voltage recording of an Fsh cell and uncaging in neighboring Lh cell.

Figure 8: Ca^{2+} responses in surrounding cells following uncaging in Lh cells. (A, B) Ca^{2+} responses in neighboring cells following uncaging in an Lh cell (green color). The laser simultaneously uncaged the Ca^{2+} and bleached the target cell, allowing verification of the precise location of the uncaging. (A) A 300 ms laser pulse targeting one Lh cell elicited a robust Ca^{2+} response in three surrounding cells. Upper panel, representative images of the response. Lower, traces of the three responses calculated as F/F_0 following background subtractions. (B) Same as (A) but only one neighbor cell responded to the uncaging. (C)

854 Overview of possible mechanisms responsible for the electrical response and the Ca^{2+}

855 response to uncaging of Ca^{2+}. Scale bars in A and B: 10 μm.

856

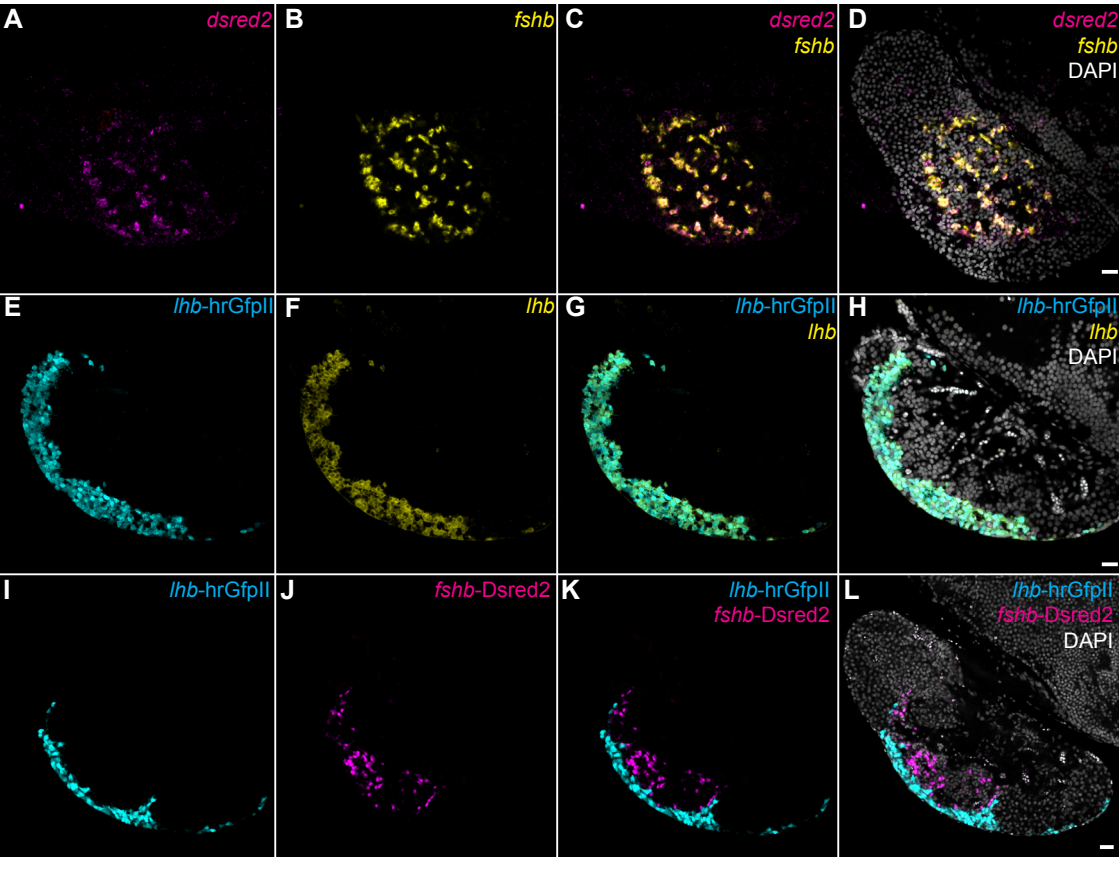
A
dsred2
B
fshb
C
dsred2
fshb
D
dsred2
fshb
DAPI
E
lhb-hrGfpII
F
lhb
G
lhb-hrGfpII
lhb
H
lhb-hrGfpII
lhb
DAPI
I
lhb-hrGfpII
J
fshb-Dsred2
K
lhb-hrGfpII
fshb-Dsred2
L
lhb-hrGfpII
fshb-Dsred2
DAPI

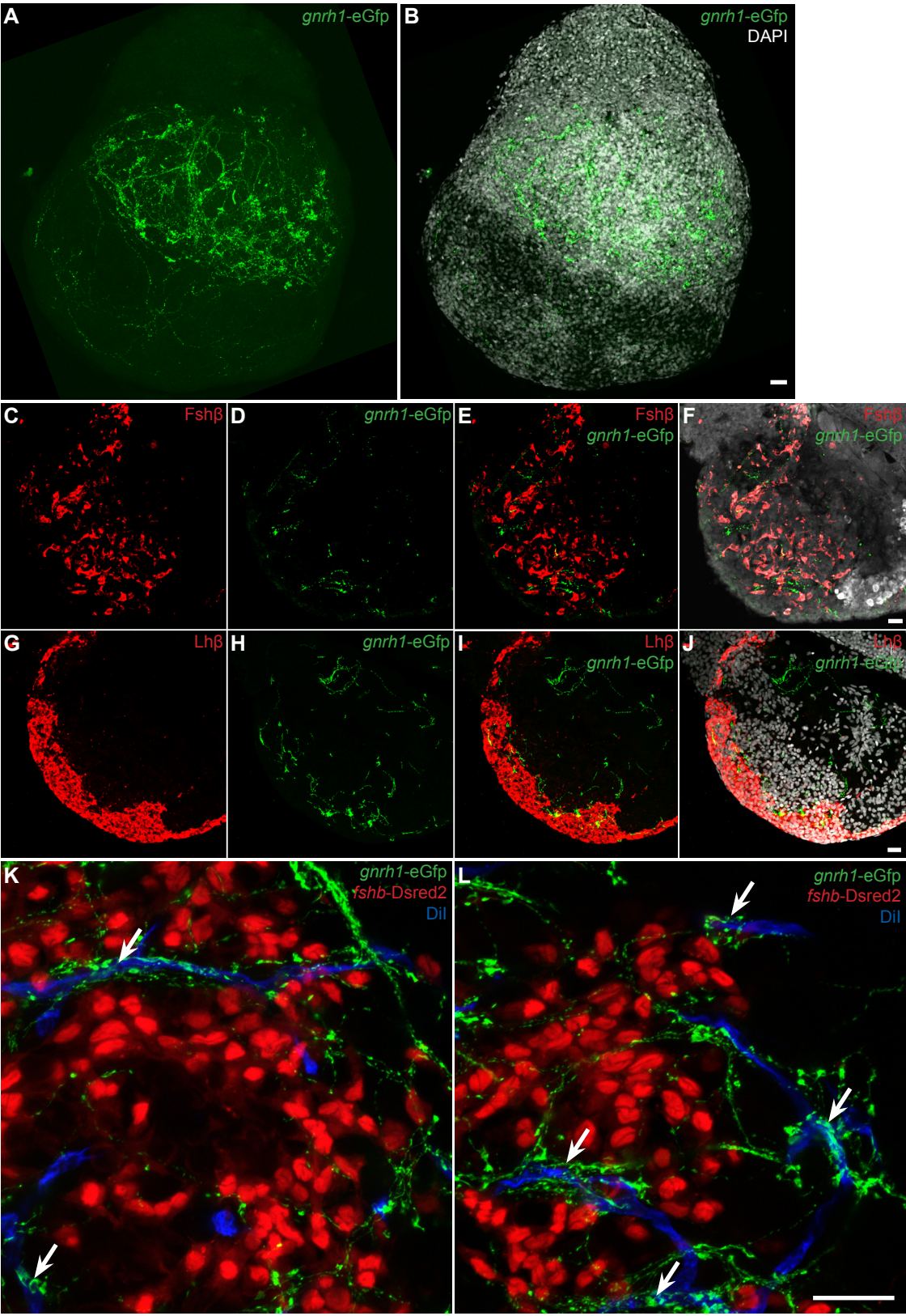
A
gnrh1-eGfp
B
gnrh1-eGfp
DAPI
C
Fshβ
D
gnrh1-eGfp
E
Fshβ
gnrh1-eGfp
F
Fshβ
gnrh1-eGfp
G
Lhβ
H
gnrh1-eGfp
I
Lhβ
gnrh1-eGfp
J
Lhβ
gnrh1-eGfp
K
gnrh1-eGfp
fshb-Dsred2
DiI
L
gnrh1-eGfp
fshb-Dsred2
DiI

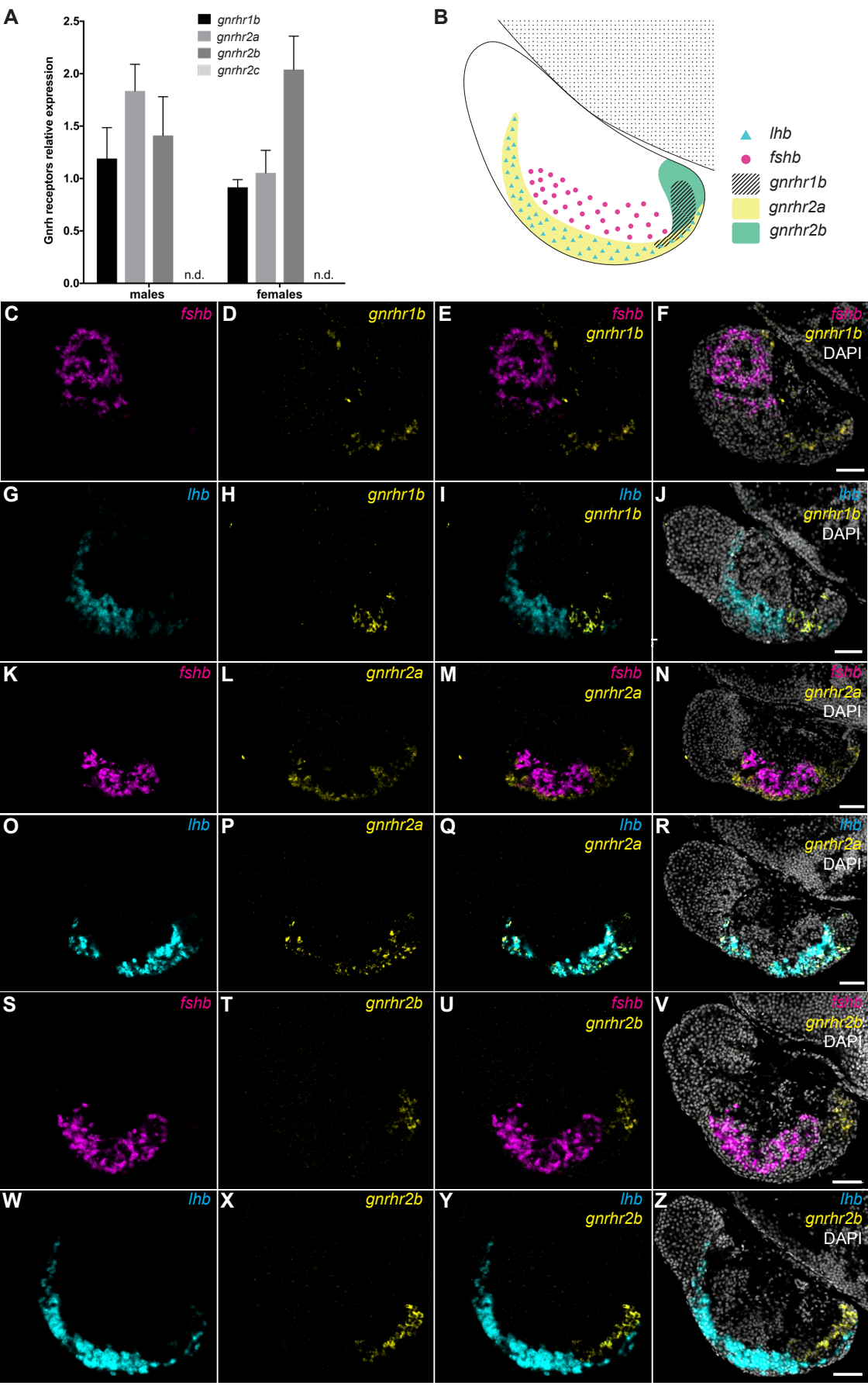
A
Gnrh receptors relative expression
2.5
2.0
1.5
1.0
0.5
0.0
gnrhr1b
gnrhr2a
gnrhr2b
gnrhr2c
n.d.
n.d.
males
females
B
lhb
fshb
gnrhr1b
gnrhr2a
gnrhr2b
C fshb
D gnrhr1b
E fshb gnrhr1b
F fshb gnrhr1b DAPI
G lhb
H gnrhr1b
I lhb gnrhr1b
J lhb gnrhr1b DAPI
K fshb
L gnrhr2a
M fshb gnrhr2a
N fshb gnrhr2a DAPI
O lhb
P gnrhr2a
Q lhb gnrhr2a
R lhb gnrhr2a DAPI
S fshb
T gnrhr2b
U fshb gnrhr2b
V fshb gnrhr2b DAPI
W lhb
X gnrhr2b
Y lhb gnrhr2b
Z lhb gnrhr2b DAPI

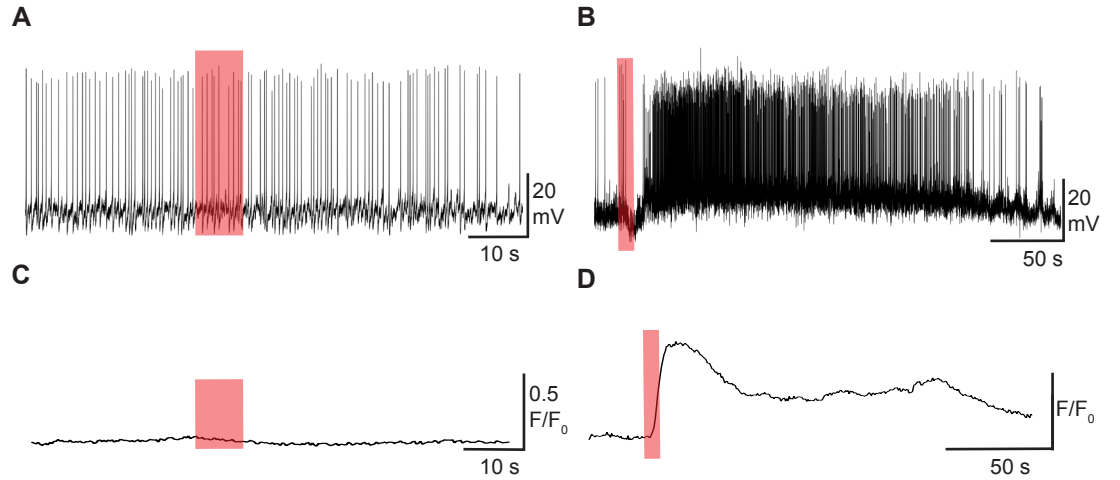
A
20
mV
10 s
B
20
mV
50 s
C
0.5
F/F0
10 s
D
F/F0
50 s

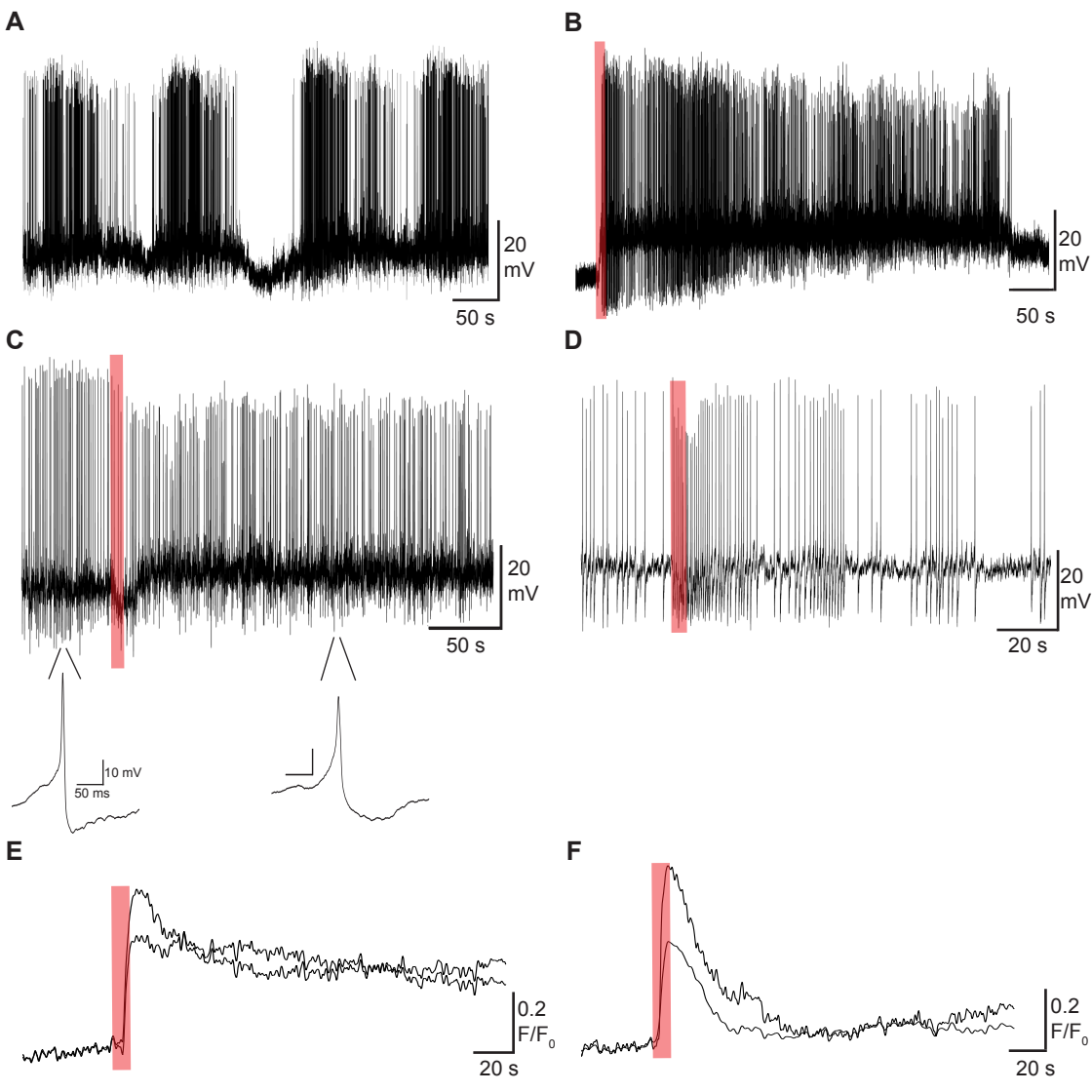
A
20
mV
50 s
B
20
mV
50 s
C
20
mV
50 s
10 mV
50 ms
D
20
mV
20 s
E
0.2
F/F0
20 s
F
0.2
F/F0
20 s

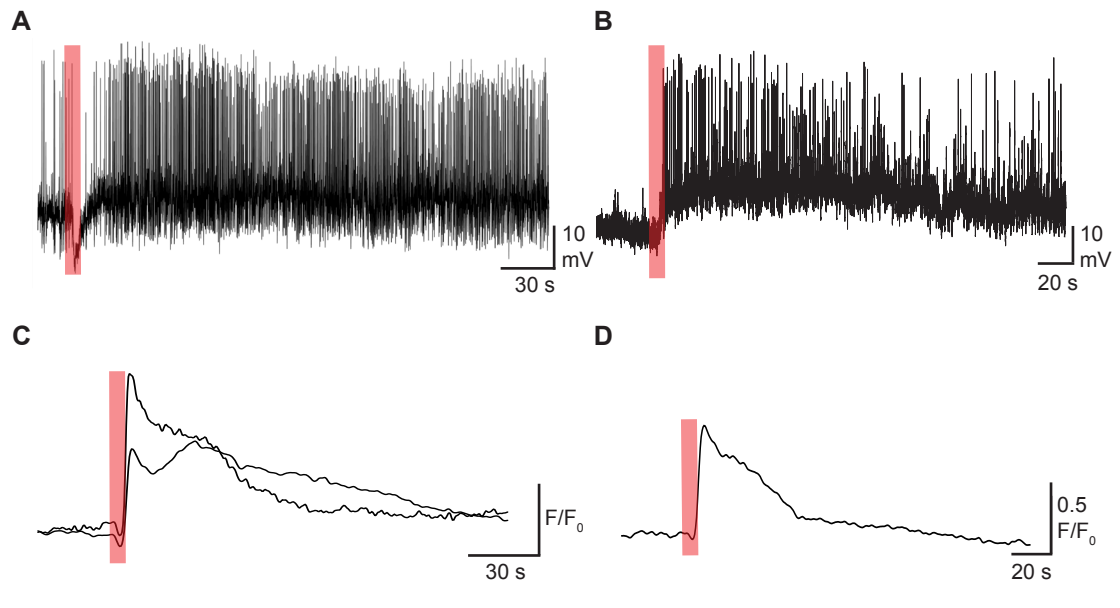
A
10
mV
30 s
B
10
mV
20 s
C
F/F0
30 s
D
0.5
F/F0
20 s

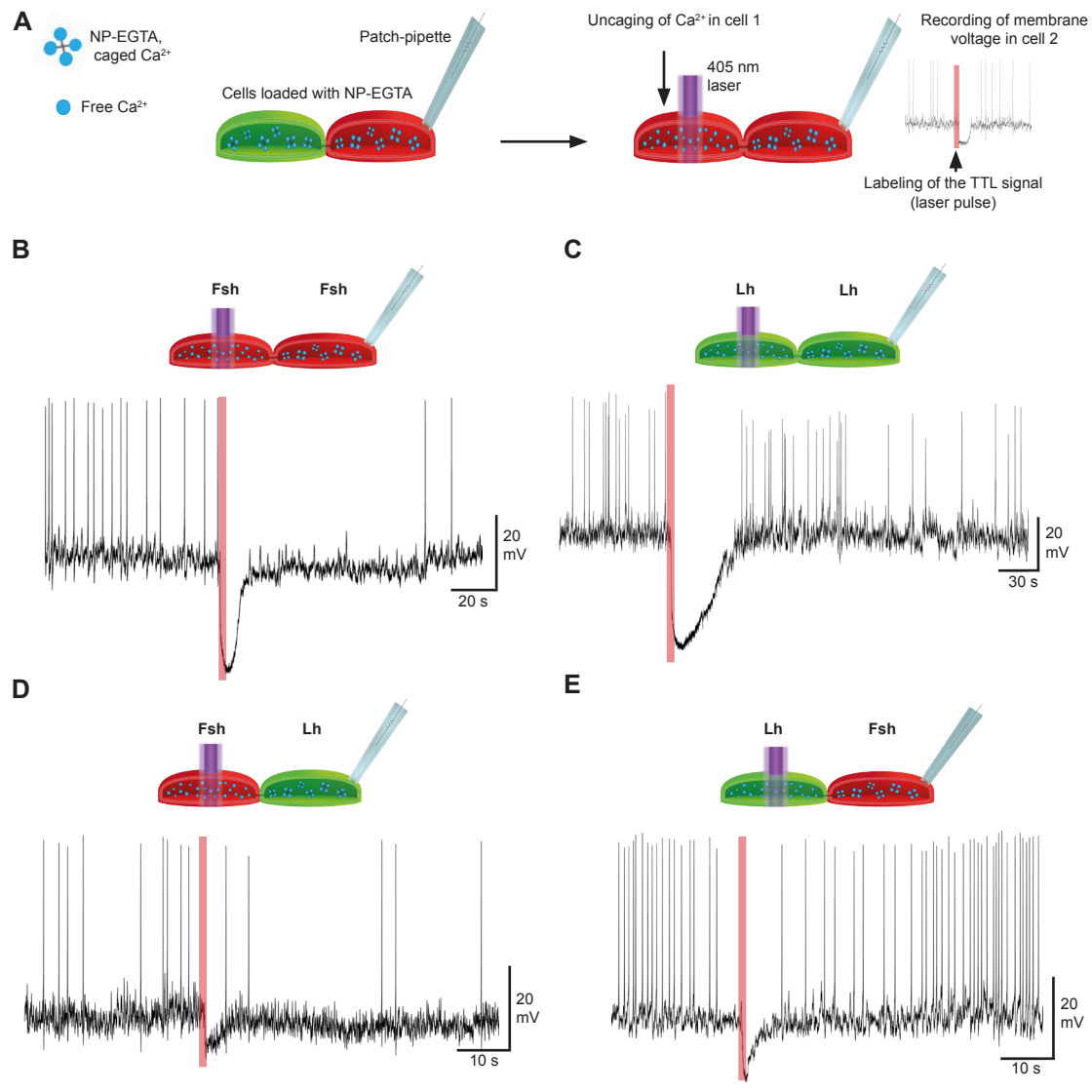
A
NP-EGTA, caged Ca2+
Free Ca2+
Patch-pipette
Cells loaded with NP-EGTA
Uncaging of Ca2+ in cell 1
405 nm laser
Recording of membrane voltage in cell 2
Labeling of the TTL signal (laser pulse)
B
Fsh
Fsh
20 mV
20 s
C
Lh
Lh
20 mV
30 s
D
Fsh
Lh
20 mV
10 s
E
Lh
Fsh
20 mV
10 s

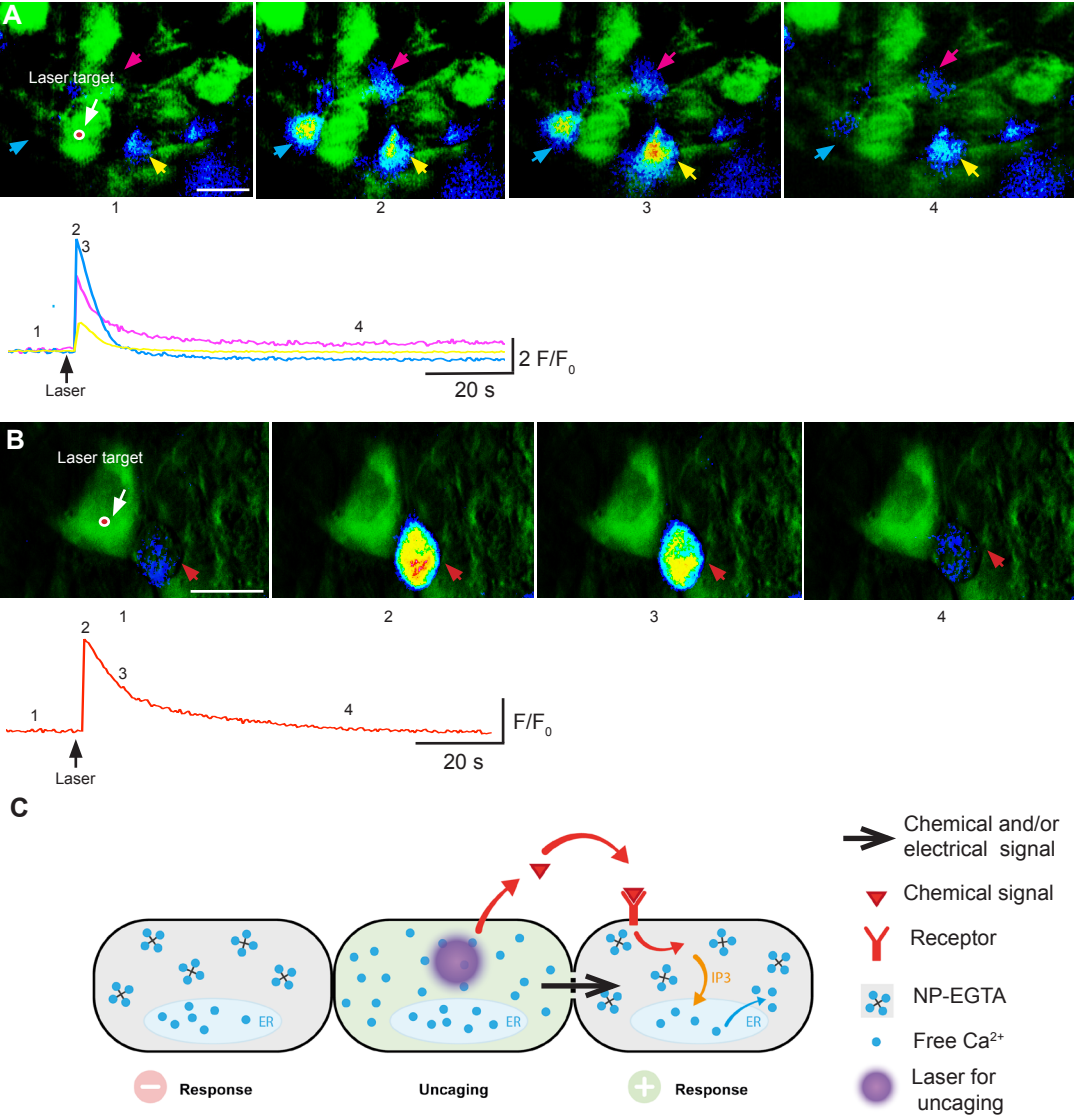
A
Laser target
1
2
3
4
2
3
1
4
Laser
2 F/F0
20 s
B
Laser target
1
2
3
4
2
3
1
4
Laser
F/F0
20 s
C
ER
ER
ER
IP3
Response
Uncaging
Response
Chemical and/or electrical signal
Chemical signal
Receptor
NP-EGTA
Free Ca2+
Laser for uncaging

Primers for cloning, qPCR and in situ

	name	forward	reverse	size of the sequence(bp)
Cloning	fshb promotor	GGCAACCTCCCTGACTGGCCTAAA	CAGTTAGCCGCCCATGCCGCTGCAG	3833
qPCR	gnrh-r1b	TCCTGCTACACATCCACCAG	GCCTTTGGGATGATGTCTGT	88
	gnrh-r2a	GGGCGATGAGTGTGATCCTC	CCCGAGTGGCACATTGAGT	96
	gnrh-r2b	TTGAGATATCAAGCCGCATC	GAGTCCTCATCCGAGCTTTG	99
	gnrh-r2c	TTCAGATCTCCAAGCAGATGAC	GGGATGTTGTTCTTTGAGCAG	79
in situ	fshb	GAGGAAGCAACACTTTCAGC	GCACAGTTTCTTTATTTCAGTGC	500
	dsred2	AGTTCATGCGCTTCAAGGTG	GTGTAGTCCTCGTTGTGGGA	598
	gnrh-r1b	CTCTTTTCTCCAGGATGACGG	TCATGCTCCCCACTGTGAG	1102
	gnrh-r2a	ATGAGCAAGCCAACATCAGC	GGCTGGACTGGTTGAGAGAT	1203
	gnrh-r2b	CGGTCTGTGGTATTGGCTTT	ACTGGCTCCTCTGGAAGTGA	876

Percentage identity

probe/mRNA	gnrh-r1b	gnrh-r2a	gnrh-r2b
gnrh-r1b	100	56.2	57.7
gnrh-r2a	56.2	100	58.2
gnrh-r2b	41.1	41.2	100